Exosomal miR-145-5p inhibits papillary thyroid cancer by targeting *TPM3* and inactivating the PI3K-Akt pathway

YUNFENG WENG[1*], XIANJIAO CAO[2*], WENYAN SONG[2] and QINGQING HE[2]

[1]Department of Thyroid and Breast Surgery, 960th Hospital of the PLA Joint Logistics Support Force, Shandong Second Medical University, Weifang, Shandong 261053, P.R. China; [2]Department of Thyroid and Breast Surgery, 960th Hospital of the PLA Joint Logistics Support Force, Jinan, Shandong 250031, P.R. China

Received June 14, 2026; Accepted August 12, 2026

DOI: 10.3892/ol.2026.15870

Abstract. Within the present study, the objective was to investigate the effects of exosomal miR-145-5p on the proliferation, migration and invasion of papillary thyroid cancer (PTC) cells, and explore the molecular mechanism involved. Bioinformatics analyses based on numerous public databases were conducted to profile the expression of microRNA (miR)-145-5p and tropomyosin 3 (*TPM3*) in PTC and explore the associations between *TPM3* expression, tumor stemness and immune infiltration. Exosomes were isolated and separately loaded with miR-145-5p mimics, miR-145-5p inhibitors or small interfering-*TPM3*. Cellular uptake assay verified that PTC cells could efficiently internalize these modified exosomes. After uptake of the exosomes, colony formation, EdU and Transwell assays were applied to assess cell proliferation, migration and invasion. Western blotting and reverse transcription-quantitative PCR were further performed to detect the expression levels of key proteins and genes involved in the PI3K-Akt signaling pathway. Results showed miR-145-5p expression was elevated in the plasma exosomes of patients with PTC but decreased in PTC tissues. *TPM3* was notably upregulated in thyroid cancer and its expression was associated with lymph node metastasis, tumor stemness and immune cell infiltration. Both miR-145-5p overexpression and *TPM3* knockdown inhibited the malignant phenotypes of PTC cells and downregulated the activity of the PI3K-Akt pathway. By contrast, miR-145-5p inhibitors reversed the above inhibitory effects. Overall, exosomal miR-145-5p suppresses PTC progression by targeting *TPM3* and inhibiting the PI3K-Akt signaling pathway. The present finding provides a novel molecular target and theoretical foundation for targeted therapy of thyroid cancer.

Correspondence to: Professor Qingqing He, Department of Thyroid and Breast Surgery, 960th Hospital of the PLA Joint Logistics Support Force, 25 Shifan Road, Jinan, Shandong 250031, P.R. China
E-mail: heqingqing@yeah.net

*Contributed equally

Key words: exosomes, miR-145-5p, papillary thyroid cancer, tropomyosin 3, PI3K-Akt

Introduction

Thyroid cancer is the most prevalent endocrine malignancy and fourth most common newly diagnosed cancer in Chinese women, as well as the seventh worldwide (1). Despite being generally indolent, ~20% of patients develop invasion, lymph node metastasis and recurrence, underscoring the urgent need for novel biomarkers and therapeutic targets (2). Exosomes mediate intercellular communication by delivering bioactive molecules that modulate malignant phenotypes; thus, they have emerged as a key focus in oncology (3-5). For example, exosomal microRNA (miR)-146b and miR-152 suppress cell proliferation and promote apoptosis, whereas exosomal miR-181a facilitates angiogenesis and tumor growth through the Yes-associated protein/VEGFR axis (6-8). This functional duality highlights the importance of understanding the precise role of individual exosomal miRNAs in papillary thyroid cancer (PTC).

The present preliminary experiments showed that plasma exosomal miR-145-5p was markedly elevated in patients with PTC compared with that in those with benign thyroid nodules, with a further increase in cases with lymph node metastasis. The present finding further highlighted a prior report of elevated exosomal miR-145-5p in PTC (9); however, it revealed a notable paradox for miR-145-5p, which is a well-established tumor-suppressive miRNA generally downregulated in cancers (10,11). The enrichment of this miRNA in circulating exosomes alongside disease progression raises an unresolved question about its functional role in PTC.

Tropomyosin 3 (*TPM3*), a predicted target of miR-145-5p as identified by TargetScan (12), is a key oncogenic factor that regulates cell morphology, motility and signal transduction (13). In thyroid cancer, *TPM3* gene fusions constitutively activate kinase receptors to drive tumorigenesis (14) and the present analysis of The Cancer Genome Atlas (TCGA) data determined its high expression and involvement in cancer stemness and immune infiltration. Furthermore, the oncogenic roles of *TPM3* have been documented in other malignancies, such as cervical cancer (15,16). Based on this predicted targeting

association and the aberrant profiles of both molecules in PTC, it was hypothesized that exosomal miR-145-5p may modulate the biological behaviors of PTC cells by targeting *TPM3*. Therefore, the present study aimed to investigate this regulatory mechanism by clarifying the functional importance of exosomal miR-145-5p in thyroid cancer.

Materials and methods

Prediction of miR-145-5p target genes. CancerMIRNome (http://bioinfo.jialab-ucr.org/CancerMIRNome), a platform that integrates TCGA database and 40 public circulating miRNome datasets, was adopted to detect differentially expressed miRNAs in thyroid cancer. TargetScan (https://www.targetscan.org/vert_80/) and mirDIP (https://ophid.utoronto.ca/mirDIP) were utilized to predict the regulatory targets of miR-145-5p and a Venn diagram was used to extract common target genes. The Database for Annotation, Visualization and Integrated Discovery (DAVID; https://www.davidbioinformatics.nih.gov/) was used for Gene Ontology (GO; https://www.geneontology.org) and Kyoto Encyclopedia of Genes and Genomes (KEGG; https://www.kegg.ip/) functional enrichment of these shared genes. The top 10 biological processes and molecular function terms were selected, as well as the top 10 KEGG pathways for visual analysis. In addition, the University of Alabama at Birmingham Cancer data analysis Portal (UALCAN; http://ualcan.path.uab.edu), a TCGA-supported analytical tool, was used to assess *TPM3* expression in tumor and non-tumor tissues.

Immune regulatory gene, immune checkpoints, tumor stemness score and immune infiltration analysis. Using The University of California, Santa Cruz (UCSC; https://genome.ucsc.edu/) database, MuTect2 software (https://gatk.broadinstitute.org/hc/en-us/articles/360037593851-Mutect2) and R software (version 4.5.1; https://www.R-project.org) the association between *TPM3* expression and five categories of immune pathway markers were analyzed, including 41 chemokines, 18 receptors, 21 major histocompatibility complex (MHC) molecules, 24 immunoinhibitors and 46 immunostimulators. Pearson's correlation analysis was performed between *TPM3* expression and 60 immune checkpoint genes (24 inhibitory and 36 stimulatory genes) extracted from the UCSC pan-cancer dataset. Tumor stemness scores (ss) were calculated using *TPM3* expression and DNAss values derived from methylation profiles. For immune infiltration analysis, *TPM3* was extracted and gene expression profiles of thyroid cancer samples from the UCSC database and mapped them to GeneSymbol (https://www.genenames.org/). The R package Estimate of Stromal and Immune cells in Malignant Tumor tissues using Expression data (ESTIMATE) (17) was used to calculate stromal, immune and ESTIMATE scores for each patient with thyroid cancer, yielding immune infiltration scores. Pearson's correlation coefficients between *TPM3* expression and immune infiltration scores in thyroid cancer were calculated using the 'corr.test' function of the R package psych (version 2.1.6; https://CRAN.R-project.org/package=psych). The Tumor Immune Estimation Resource (TIMER) database (18) was further used to evaluate immune cell infiltration levels in thyroid cancer, based on the integrated algorithms of Tumor Immune Dysfunction and Exclusion (TIDE), Estimating the Proportions of Immune and Cancer cells (EPIC) (19), Microenvironment Cell Populations (MCP)-counter, Cell-type Identification By Estimating Relative Subsets of RNA Transcripts (CIBERSORT) (20), CIBERSORT-absolute mode (ABS) and xCell (21).

Cell culture. Human umbilical cord mesenchymal stem cells (hUC-MSCs) were isolated from Wharton's jelly of discarded umbilical cords obtained from 5 healthy pregnant donors between September 3rd and September 18th 2024, at the 960th Hospital of the PLA Joint Logistics Support Force (Jinan, China). The present study was approved by the Ethics Committee of the 960th Hospital of the PLA Joint Logistics Support Force (approval no. 2024 044) and written informed consent was obtained from all donors prior to sample collection. After removal of umbilical arteries and veins, the gelatinous connective tissue was minced into 5-10 mm^3 fragments, adhered to T75 flasks for 1 h at 37˚C and cultured in 15 ml serum-free complete medium (Mele Biotech). Successful isolation of hUC-MSCs was determined by morphological observation and flow cytometric phenotyping: The cells displayed typical spindle-shaped, adherent growth with fascicular/swirling arrangements and were positive for CD73, CD90, and CD105 (>90%) while negative for CD34 and CD45 (<2%). Thyroid papillary carcinoma (TPC)-1 cells (Wuhan Servicebio Technology Co., Ltd.) were maintained in RPMI-1640 medium (Procell Life Science & Technology Co., Ltd.) supplemented with 10% FBS, 100 U/ml penicillin and 100 μg/ml streptomycin at 37˚C in 5% CO_2.

Exosome extraction. Exosomes were purified from the supernatant of hUC-MSCs using an ultracentrifugation method. The plasma and cell supernatant were first centrifuged at 300 x g for 10 min at 4˚C to remove precipitates and the resulting supernatant was collected and further centrifuged at 10,000 x g for 30 min at 4˚C. After supernatant collection, ultracentrifugation was performed at 120,000 x g for 90 min at 4˚C. The final pellet was resuspended in PBS, and the purified exosomes were prepared for subsequent experiments.

Exosome identification. Isolated exosomes were fixed with 4% paraformaldehyde at room temperature for 10 min and dropped onto 300-mesh carbon-coated copper grids. After staining with 2% uranyl acetate aqueous solution (Mele Biotech) at room temperature for 90 sec, morphological characteristics of the exosomes were observed and imaged using transmission electron microscopy (TEM; ZetaView-PMX120-Z; version 8.04.02 SP2; Particle Metrix GmbH). For exosome identification, western blotting analysis was performed to detect the expression of exosomal marker proteins including TSG101 (1:1,000 dilution; cat. no. 67381-1-PBS; Proteintech Group, Inc.), CD9 (1:1,000 dilution; cat. no. 20597-1-AP; Proteintech Group, Inc.) and CD81 (1:1,000 dilution; cat. no. 66866-1-Ig; Proteintech Group, Inc.) following the same procedure as described in the western blotting subsection.

Exosomal miRNA transfection experiment. Exosomal miRNA transfection was performed using an Exosomal Small RNA Nucleic Acid Loading kit (cat. no. E0051; Mele Biotech) following the manufacturer's protocol. Briefly, 30 pmol

Table I. Sequences of miRNA mimics, inhibitor, siRNA and NCs.

Name	Sense/antisense	Oligonucleotide sequence (5'-3')
miR-145-5p mimics	Sense	GUCCAGUUUUCCCAGGAAUCCCU
	Antisense	AGGGAUUCCUGGGAAAACUGGAC
miR-145-5p NC	Sense	UCACAACCUCCUAGAAAGAGUAGA
	Antisense	UCUACUCUUUCUAGGAGGUUGUGA
miR-145-5p inhibitor	NA	AGGGAUUCCUGGGAAAACUGGAC
si-TPM3	Sense	UAAGAAUCUUGAUUUCUUCCU
	Antisense	GAAGAAAUCAAGAUUCUUACU
si-NC	Sense	UUCUCCGAACGUGUCACGU
	Antisense	ACGUGACACGUUCGGAGAA

miR, microRNA; si, small interfering; TPM3, tropomyosin 3; NC, negative control; NA, not applicable.

miR-145-5p mimics, miR-145-5p inhibitor, miR-145-5p NC, small interfering (si)-*TPM3* and si-NC (GenCefe Biotech) were individually mixed with EXO-fect reagent in 25 μl Trans solution (Mele Biotech). After 5 min incubation at room temperature, the corresponding mixtures were combined and incubated for another 15 min at room temperature to form transfection complexes. Subsequently, 150 μl exosomes derived from the hUC-MSCs were added to the transfection complexes. The mixture was subjected to ultrasonic treatment (110 W, 6 sec ultrasound/10 sec interval and 8 cycles; Scientz-IID; Ningbo Scientz Biotechnology Co., Ltd.) and incubated overnight at 4˚C. The next day, 200 μl exosome mixture was loaded onto a spin column. After 2 min of room-temperature standing, the column was centrifuged at 1,000 x g at room temperature for 1 min to eliminate unbound free RNA, yielding target RNA-loaded modified exosomes. The sequences of all oligonucleotides used for transfection are listed in Table I.

Exosomal miR-145-5p uptake assay. TPC-1 cells were seeded on coverslips in 24-well plates. Upon reaching ~60% confluence, the cells were starved overnight in serum-free medium. After starvation, 100 μl miR-145-5p exosomes were added for 24 h incubation. The culture medium was then discarded, and the cells were rinsed three times with PBS. Nuclei of the cells were stained with 200 μl DAPI working solution at room temperature for 15 min, followed by three PBS washes. Coverslips were mounted on slides with anti-fade reagent and visualized using a fluorescence microscope (UltraVIEW VoX; PerkinElmer, Inc.).

Colony formation assay. Exosome-treated cells were seeded into six-well plates at a density of $1x10^3$ cells per well and cultured for 10 days. Subsequently, the cells were fixed with 4% paraformaldehyde at room temperature for 15 min and stained with 0.1% (w/v) crystal violet at room temperature for 20 min. Colonies, defined as visible cell clusters stained with crystal violet that contained at least 50 cells, were counted manually and imaged.

EdU assay. Exosome-treated cells were seeded in 24-well plates at a density of $5x10^3$ cells per well and cultured for 24 h. Subsequently, EdU reagent (cat. no. C0071S; Beyotime Biotechnology) was added to each well at a final concentration of 10 μM and the cells were incubated for another 2 h at 37˚C. The cells were then incubated with Click reaction reagent (Beyotime Biotechnology) for 30 min at room temperature in the dark. After removal of the reaction solution, the cells were thoroughly washed with Immunol Staining Wash Buffer (Beyotime Biotechnology). Nuclei of the cells were counterstained with Hoechst 33342 (1 μg/ml) at room temperature for 30 min in the dark, followed by PBS rinsing. EdU-positive (green fluorescence) and Hoechst 33342-positive (blue fluorescence) cells were observed and counted under a fluorescence microscope (Olympus BX53; Olympus Corporation).

Transwell migration and invasion assays. For the invasion assay, Matrigel (Corning, Inc.) was diluted with serum-free culture medium at a ratio of 1:5 and 100 μl of the diluted Matrigel was coated onto Transwell inserts (8-μm pore size; Corning, Inc.). The inserts were placed in an incubator at 37˚C for 2 h to allow gel solidification. Exosome-treated cells were trypsinized, resuspended in serum-free medium, seeded into the inserts at a density of $2x10^4$ cells per well in 100 μl of complete medium containing 10% FBS (600 μl) was added to the lower chamber. After 24 h of culture at 37˚C in a 5% CO_2 incubator, the inserts were collected, fixed with 4% paraformaldehyde (500 μl) at room temperature for 15 min, and stained with 0.1% (w/v) crystal violet solution (500 μl) at room temperature for 20 min. The cells remaining on the upper membrane were removed and invasive cells on the lower membrane were imaged by inverted light microscope (OLYMPUS CKX41; Olympus Corporation) and cell counting was performed manually. The migration assay was performed following the same procedures without Matrigel coating.

Western blotting. Total proteins were extracted from cell lysates or exosomes. For exosome samples were lysed in RIPA lysis buffer (Mele Biotech) supplemented with 1% PMSF on ice for 30 min. Protein concentrations were determined using a BCA protein assay kit (Beyotime Biotechnology), and equal amounts of protein (20 μg per lane) were separated using 10% SDS-PAGE (Beyotime Biotechnology). Subsequently, the proteins were transferred onto PVDF membranes. All

Table II. Primer sequences.

Gene	Direction	Primer sequence (5'-3')
TPM3	Forward	GACTTGGAACGCACAGAGGAAC
	Reverse	AAGAGACTTGAGGTTGTTGGTGAC
PI3K	Forward	TATGGTTGTCTGTCAATCGGTGA
	Reverse	GCCTTTGCAGTGAATTTGCAT
Akt	Forward	GTGCTGGAGGACAACGACT
	Reverse	GTGTAGGGTCCTTCTTGAGCA
GAPDH	Forward	TCCAAAATCAAGTGGGGCGA
	Reverse	AAATGAGCCCCAGCCTTCTC
miR-145-5p	RT primer	CTCAACTGGTGTGGTGGAGTCGGCAATTCAG TTGAGAGGGATTC
	Forward	ACACTCCAGCTGGGGTCCAGTTTTCCCAGGA
U6	Universal reverse	TGGTGTCGTGGAGTCG
	Forward	CTCGCTTCGGCAGCACA
	Reverse	AACGCTTCACGAATTTGCGT

miR, microRNA; TPM3, tropomyosin 3; RT, reverse transcription.

primary and secondary antibodies were diluted at a ratio of 1:1,000. The membranes were blocked with 5% non-fat milk in TBST at room temperature for 1 h and the membranes were incubated overnight at 4˚C with primary antibodies against TPM3 (cat. no. DF6338; Affinity Biosciences), PI3K p110 (cat. no. A19742; ABclonal Biotech Co., Ltd.), PI3K p85 (cat. no. A4992; Abclonal Biotech Co., Ltd.), Akt (cat. no. A29131; Abclonal Biotech Co., Ltd.) and p-Akt (cat. no. AP0637; Abclonal Biotech Co., Ltd.). The membranes were then incubated with corresponding HRP-conjugated anti-rabbit secondary antibodies (cat. no. AS029; ABclonal Biotech Co., Ltd.) at room temperature for 1 h and protein bands were visualized using enhanced chemiluminescence reagent (Beyotime Biotechnology). For membrane stripping and re-probing, the membranes were treated with antibody stripping solution (Beyotime Biotechnology), re-blocked and incubated with β-tubulin primary antibody (1:1,000 dilution; cat. no. ET1602-4; HUABIO). The remaining procedures were consistent with the aforementioned steps.

Reverse transcription-quantitative PCR (RT-qPCR). Total cellular RNA was extracted using an RNA purification kit (cat. no. AC0202; Shandong Sparkjade Scientific Instruments Co., Ltd). For mRNA detection, RNA was reverse-transcribed into cDNA using a reverse transcription kit (cat. no. AG0302; Shandong Sparkjade Scientific Instruments Co., Ltd.) with oligo primers according to the manufacturer's protocol, and GAPDH was used as the internal reference. For miRNA detection, specific stem-loop reverse transcription primers were used and U6 was used as the internal reference. The expression levels were quantified through RT-qPCR using SYBR Green qPCR Mix (cat. no. AG0305; Shandong Sparkjade Scientific Instruments Co., Ltd) according to manufacturer's protocol. The thermocycling conditions were as follows: Initial denaturation at 94˚C for 2 min, followed by 40 cycles of 94˚C for 5 sec and 60˚C for 30 sec, with a dissociation stage for melt curve analysis. The relative gene expression levels were calculated using the $2^{-\Delta\Delta Cq}$ method (22). All primer sequences are listed in Table II.

Statistical analysis. All data are presented as the mean ± SD. Statistical comparisons between two groups were performed using unpaired two-tailed Student's t-test. Multiple group comparisons were conducted using one-way analysis of variance followed by the Tukey's post-hoc test. $P<0.05$ was considered to indicate a statistically significant difference. All the experiments were repeated independently at least three times.

Results

Role of miR-145-5p in PTC. To clarify the biological role of miR-145-5p in thyroid cancer, its expression was first examined using TCGA data. Compared with normal tissues, miR-145-5p was notably downregulated in thyroid cancer tissues (Fig. 1A). To explore its potential regulatory mechanisms, target genes were predicted by intersecting the results from TargetScan and mirDIP databases (Fig. 1B). KEGG pathway enrichment analysis revealed that these overlapping target genes were notably enriched in tumor-associated pathways, including the 'MAPK signaling pathway', 'Rap1 signaling pathway' and 'TGF-β signaling pathway' (Fig. 1C), suggesting that miR-145-5p may modulate thyroid cancer progression by regulating these pathways.

GO biological process analysis showed that the target genes were primarily involved in 'response to transforming growth factor β', 'Ras protein signal transduction' and the 'transmembrane receptor protein serine/threonine kinase signaling pathway' (Fig. 1D). Molecular function analysis further revealed notable enrichment in functions associated with 'GTPase regulator activity' and 'GTPase activator activity' (Fig. 1E). Collectively, this indicates that miR-145-5p may participate in thyroid cancer biology by mediating cytoskeletal remodeling and responses to cellular signals. Based on

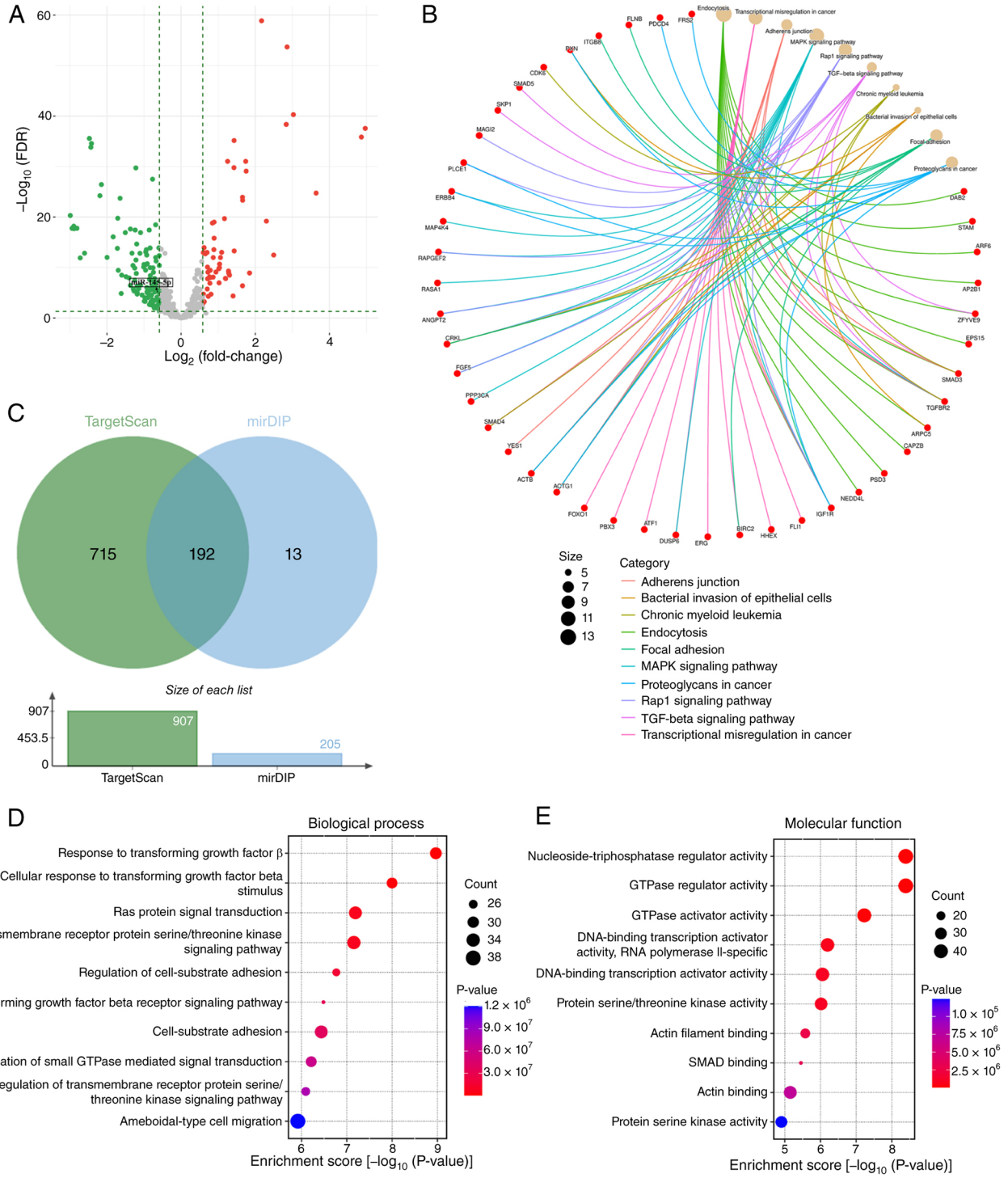

Figure 1. Differential expression and functional analysis of miR-145-5p. (A) Volcano plot of differentially expressed miRNAs in thyroid cancer, in which miR-145-5p is indicated in the green region on the left. (B) Kyoto Encyclopedia of Genes and Genomes pathway enrichment. (C) Venn diagram showing the intersection of miR-145-5p target genes predicted by TargetScan and mirDIP databases. (D) Gene Ontology-biological processes and (E) Gene Ontology-molecular functions functional enrichment analyses performed based on the intersected target genes. miR, micro-RNA; FDR, false discovery rate.

the enrichment results, *TPM3* was selected as the core target gene for further validation. Analysis using multiple prediction databases indicated that miR-145-5p could complementarily bind to the 3' untranslated region of *TPM3*.

High expression of TPM3 mRNA in thyroid cancer. To further investigate the role of *TPM3* in thyroid cancer progression, its transcriptomic expression was analyzed using the UALCAN database. *TPM3* mRNA levels were found to be significantly higher in thyroid cancer tissues compared with those in normal tissues (normal vs. primary: P<0.001; Fig. 2A). In addition, elevated *TPM3* expression was evident across different clinical stages (normal vs. stage 2, 3 4; P<0.01; Fig. 2B). Among thyroid cancer subtypes, classic PTC exhibited the highest *TPM3* expression (normal vs. classical PTC: P<0.01; normal vs. tall PTC: P<0.05; Fig. 2C). Moreover, *TPM3* expression was

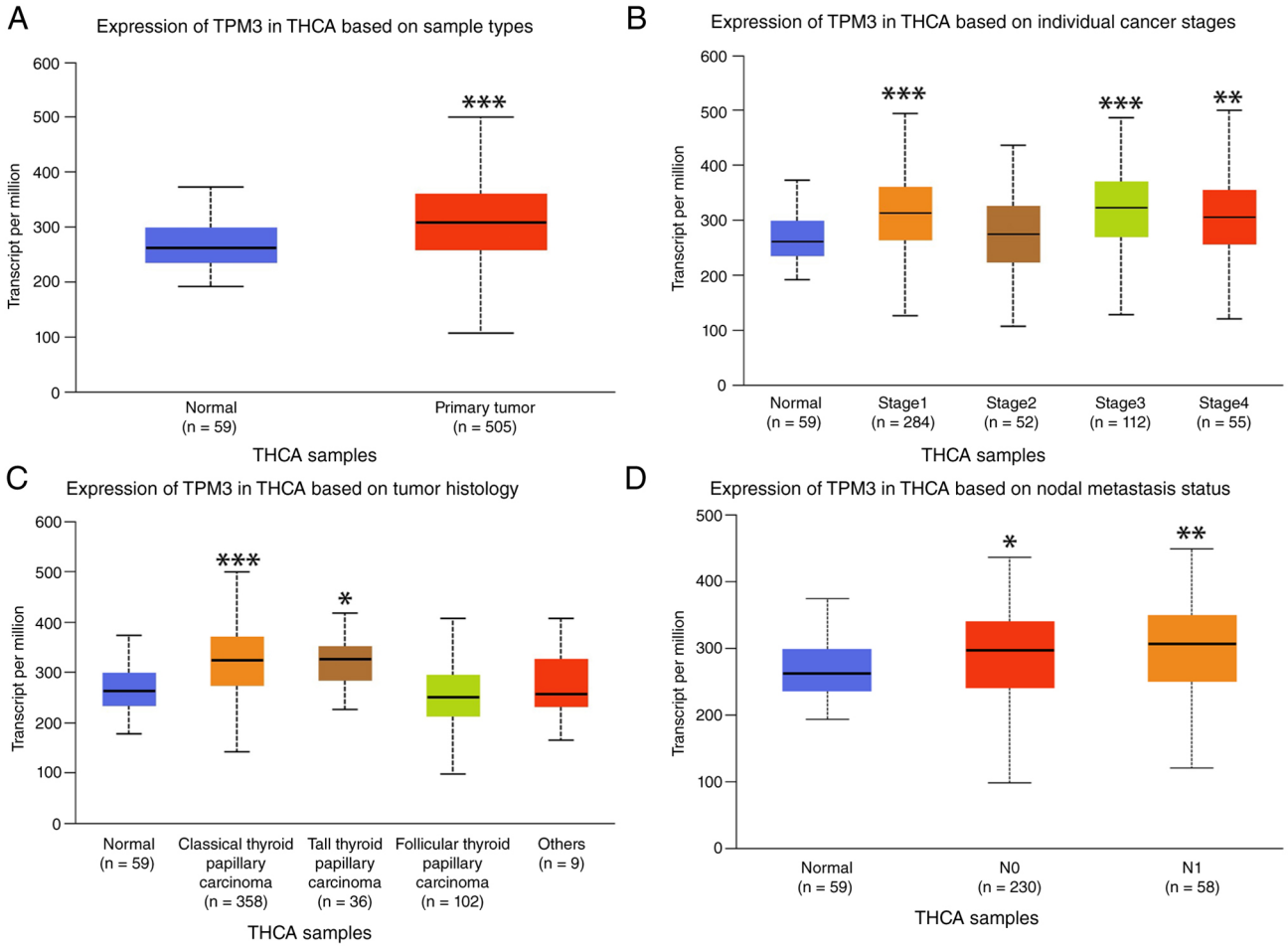

Figure 2. Analysis of *TPM3* mRNA expression level in thyroid cancer tissues based on The Cancer Genome Atlas database. (A) mRNA levels of *TPM3* in thyroid cancer and normal tissues. (B) mRNA levels of *TPM3* in thyroid cancer at different clinical stages. (C) mRNA levels of *TPM3* in different types of thyroid cancer. (D) mRNA levels of *TPM3* in thyroid cancer with and without lymph node metastasis. *P<0.05, **P<0.01 and ***P<0.001 vs. normal. TPM3; tropomyosin 3; THCA, thyroid carcinoma.

significantly associated with lymph node metastasis (normal vs. N0: P<0.05; normal vs. N1: P<0.01; Fig. 2D). Notably, in thyroid cancer, *TPM3* was upregulated while miR-145-5p was downregulated, demonstrating opposing expression patterns. This reciprocal association suggests that miR-145-5p may be involved in thyroid cancer progression through negative *TPM3* regulation.

Correlation between TPM3 expression and immune regulatory genes. To explore the role of *TPM3* in tumor immune regulation, its correlation with immune regulatory genes, immune checkpoints, tumor stemness scores and immune infiltration levels were analyzed. *TPM3* expression data and 150 marker genes from five immune pathways, including chemokine (n=41), receptor (n=18), MHC (n=21), immunoinhibitor (n=24) and immunostimulator (n=46), were extracted from the pan-cancer dataset downloaded from the UCSC database. Pearson's correlation analysis revealed that *TPM3* expression was positively correlated with majority of these immune regulatory genes in thyroid cancer (Fig. 3A). Further analysis of immune checkpoints, including inhibitory (n=24) and stimulatory (n=36) molecules, demonstrated that *TPM3* also showed significant correlations with the majority of immune checkpoints (Fig. 3B). In addition, *TPM3* expression was shown to be significantly positively correlated with tumor stemness (Fig. 4A) and immune infiltration (Fig. 4B) scores in thyroid cancer.

TIMER2 was further used to examine the association between *TPM3* expression and immune cell infiltration levels across all the TCGA cancer types, using multiple evaluation algorithms including TIDE, EPIC, MCP-counter, CIBERSORT, CIBERSORT-ABS and xCell. In thyroid cancer, *TPM3* expression was shown to be positively correlated with the infiltration of regulatory T cells (Tregs), natural killer (NK) T cells, common lymphoid progenitor cells and cancer-associated fibroblasts (CAFs), whereas it was negatively correlated with infiltration of myeloid-derived suppressor and endothelial cells (Fig. 4C).

Roles of exosomal miR-145-5p in PTC cells. To investigate whether miR-145-5p could be delivered into PTC cells via exosomes, exosomes were isolated from the culture supernatant of hUC-MSCs. TEM revealed the typical cup-shaped morphology of the isolated exosomes and the mean diameter was 139.6±50.4 nm, consistent with the expected size range of exosomes (23) (Fig. 5A). Western blotting analysis determined the presence of exosomal marker proteins (CD9, CD81 and TSG101; Fig. 5B).

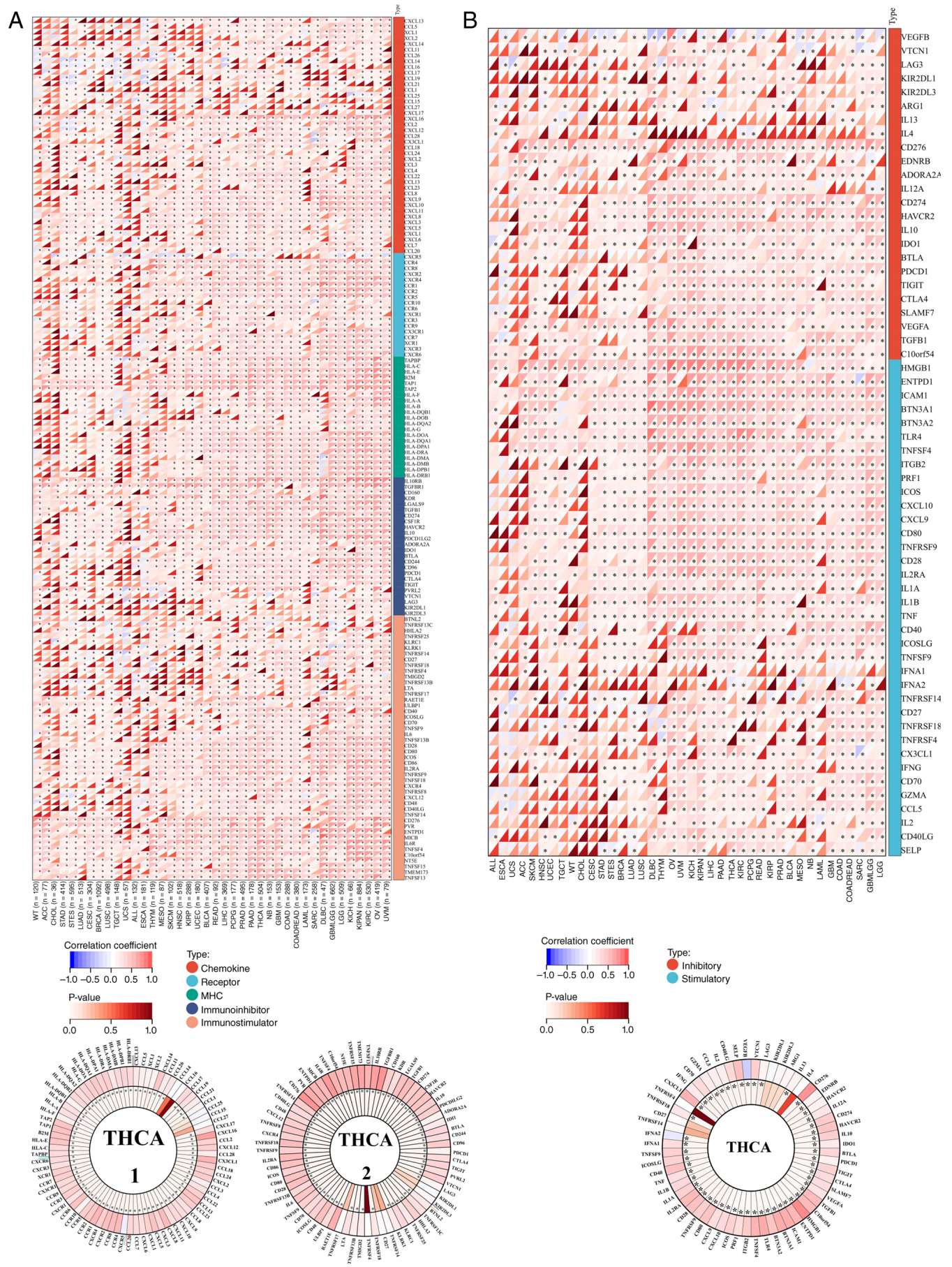

Figure 3. Correlation analysis of *TPM3* and immune regulatory genes and immune checkpoints. (A) Correlation of *TPM3* expression with most immune regulatory gene. (B) Correlation of *TPM3* and known immune checkpoints across all The Cancer Genome Atlas cancers. TPM3, tropomyosin 3; MHC, major histocompatibility complex; THCA, thyroid carcinoma.

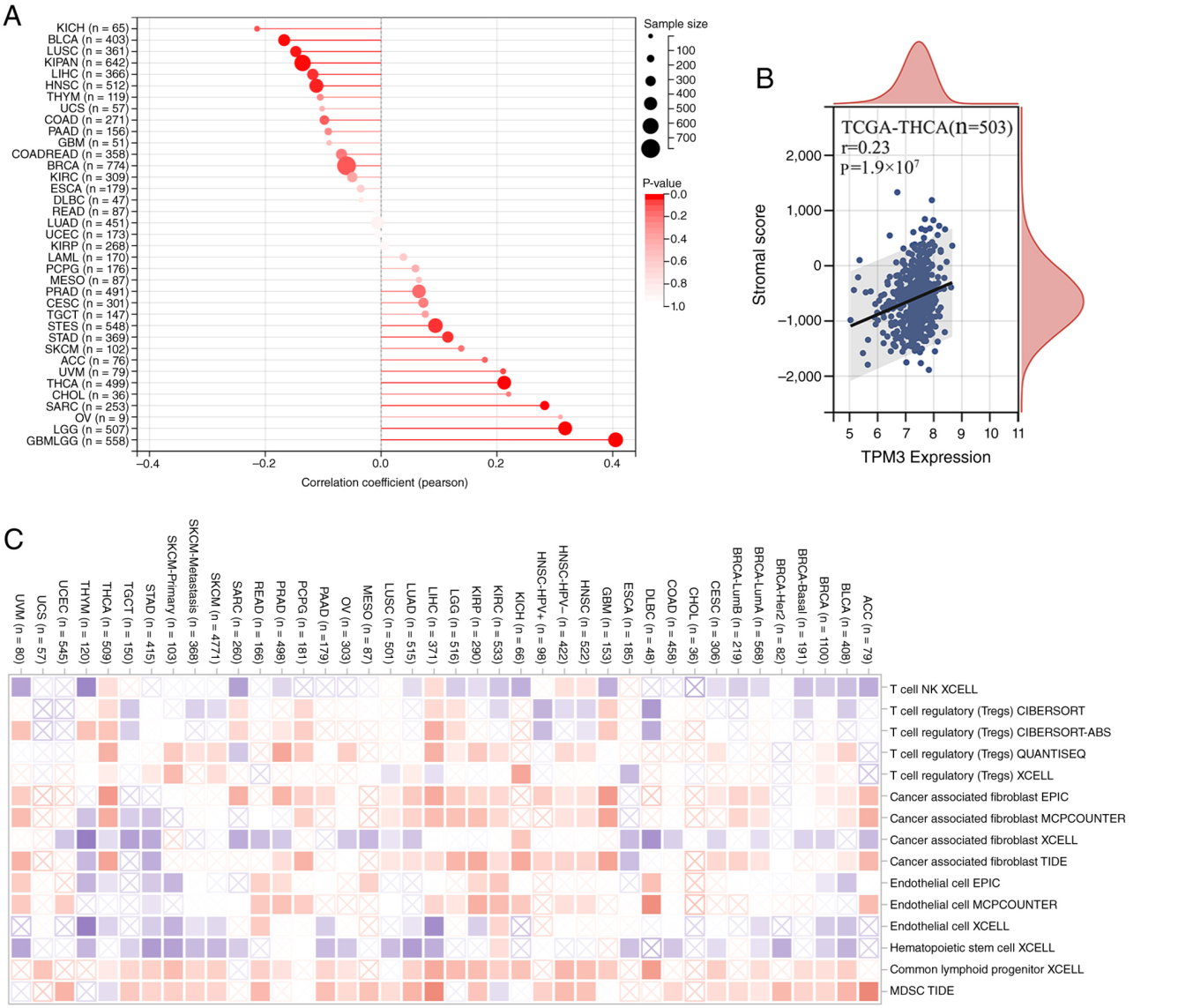

Figure 4. Tumor stemness score and immune infiltration analysis. (A) *TPM3* tumor stemness score. (B) Analysis of *TPM3* expression and immune infiltration scores in thyroid cancer. (C) Examining the correlations between *TPM3* expression and immune infiltration across all The Cancer Genome Atlas cancers using Tumor Immune Estimation Resource 2 algorithms. TPM3, tropomyosin 3; THCA, thyroid carcinoma; NK, natural killer; Treg, T regulatory cell; CIBERSORT, Cell-type Identification By Estimating Relative Subsets of RNA Transcripts; MCP-counter, Microenvironment Cell Populations-counter; CIBERSORT-ABS, CIBERSORT-Absolute Mode.

FITC-labeled miR-145-5p mimics were loaded into exosomes using an exosome transfection kit. After removing unencapsulated miR-145-5p, the loaded exosomes were co-cultured with TPC-1 cells for 24 h. Fluorescence microscopy results showed that the green fluorescence of FITC-miR-145-5p accumulated around the DAPI-stained nuclei (blue; Fig. 5C), indicating that TPC-1 cells internalized the exosomal miR-145-5p.

miR-145-5p targets TPM3 to inhibit proliferation, invasion and migration of PTC. In the colony formation assay, the colony number decreased to 63.20±6.82% (P<0.05) in the miR-145-5p mimics group and 67.44±7.52% (P<0.05) in the si-*TPM3* group but increased to 126.00±8.40% (P<0.05) in the miR-145-5p inhibitors group, compared with the NC group (Fig. 5D). Similarly, EdU proliferation assays showed that the percentage of EdU-positive cells was notably reduced to 47.31±3.23% (P<0.05) and 46.29±1.78% (P<0.05) in the mimics and si-*TPM3* groups, respectively, whereas no marked change was observed in the inhibitors group (Fig. 5E).

In the Transwell migration assay, compared with the miR-NC group, the number of migrated cells decreased to 47.31±8.34% (P<0.05) of the control in the miR-145-5p mimics group, while it increased to 133.50±16.37% (P<0.05) of the control in the inhibitors group; compared with the si-NC group, the si-*TPM3* group decreased to 61.66±4.21% (P<0.05) of the control (Fig. 6A). Consistent results were obtained in the invasion assay. Compared with the miR-NC group, the number of invaded cells decreased to 63.77±15.92% (P<0.05) of the control in the mimics group and increased to 154.30±33.36% (P<0.05) of the control in the inhibitors group. Compared with the si-NC group, the si-*TPM3* group decreased to 69.33±17.43% of the control (Fig. 6B). Collectively, these results indicate that miR-145-5p inhibits the proliferation, migration and invasion of PTC cells by targeting *TPM3*.

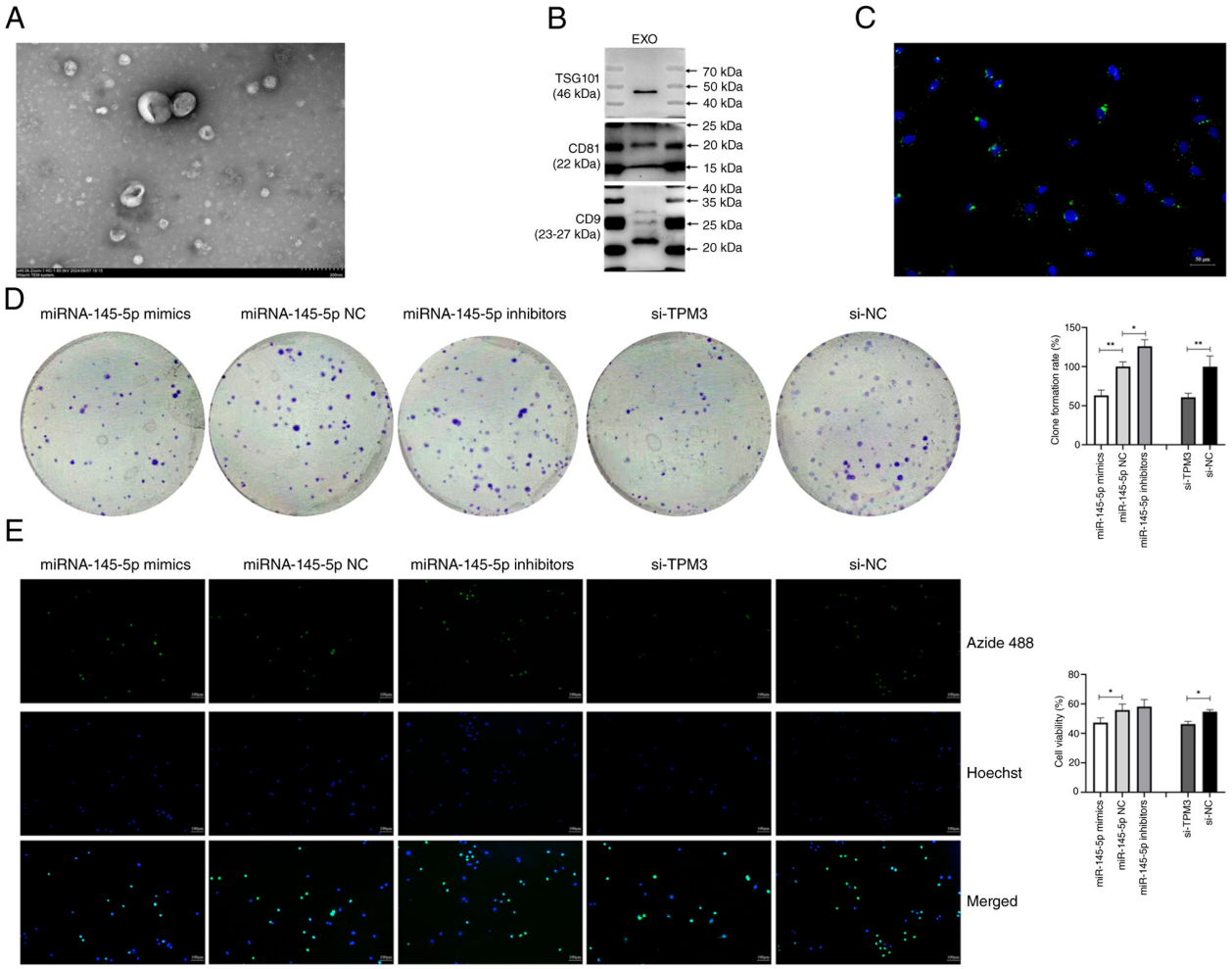

Figure 5. Effects of exosomal miR-145-5p uptake and treatment on the proliferation of papillary thyroid cancer cells. (A) Morphology of exosomes observed by transmission electron microscopy. (B) Western blotting analysis showing expression of exosomal marker proteins TSG101, CD81 and CD9. (C) Fluorescence images showing the uptake of exosomal miR-145-5p mimics-FITC by TPC-1 cells. (D) Cell proliferation detected by colony formation assay. (E) Cell proliferation assessed using EdU staining. *P<0.05 and **P<0.01 miR-145-5p mimics/inhibitors group vs. miR-145-5p NC group; si-*TPM3* group vs. si-NC group. EXO, exosome; TPC, thyroid papillary carcinoma; miR, microRNA; si, small interfering; NC, negative control; TPM3, tropomyosin 3.

miR-145-5p targets TPM3 to suppress the PI3K-Akt signaling pathway in PTC cells. Western blotting and RT-qPCR analyses were performed to evaluate the regulatory effects of miR-145-5p on downstream signaling. Western blotting results showed that, relative to the NC group, the protein levels of TPM3, PI3K, Akt and p-Akt were significantly decreased in the miR-145-5p mimics group, whereas *TPM3* and p-Akt expression was increased in the miR-145-5p inhibitors group. The expression of *TPM3*, *PI3K p85α* and p-*Akt* was significantly lower in the si-*TPM3* group compared with that in the si-NC group. Consistently, RT-qPCR data determined that the mRNA levels of PI3K and Akt were also reduced in both the mimics and si-*TPM3* groups compared with their respective controls (Fig. 6C and D). Collectively, the present findings indicate that miR-145-5p inhibits the PI3K-Akt signaling pathway by targeting *TPM3* in PTC cells.

Discussion

Despite the majority of thyroid cancers exhibiting favorable prognosis (24), with 10-year overall survival rates >90% for certain subtypes, certain refractory subtypes remain clinically challenging. Given the low proportional incidence of aggressive variants, they are the leading cause of thyroid cancer-associated mortality and poor overall survival (25). For instance, ~10% of differentiated thyroid cancers eventually develop radioiodine resistance, a condition associated with a poor prognosis, with a 10-year survival rate of only 10% from the time of metastasis detection. Therefore, to overcome current treatment limitations, novel therapeutic strategies are needed. Tumor initiation and progression are complex biological processes governed by a number of factors, including genetic mutations (such as the activation of proto-oncogenes and the inactivation of tumor suppressor genes), dynamic modulation by the tumor microenvironment and multistage mechanisms, which depend not only on the intrinsic stemness properties of tumor cells but also on dynamic modulation by the tumor microenvironment. As important mediators of intercellular communication within the tumor microenvironment, exosomes serve pivotal regulatory roles in core oncological processes, including proliferation, invasion, metastasis and angiogenesis in thyroid cancer (26). Despite this, the functional roles and underlying mechanisms of specific exosomal miRNAs in PTC remain largely unexplored. The present study systematically

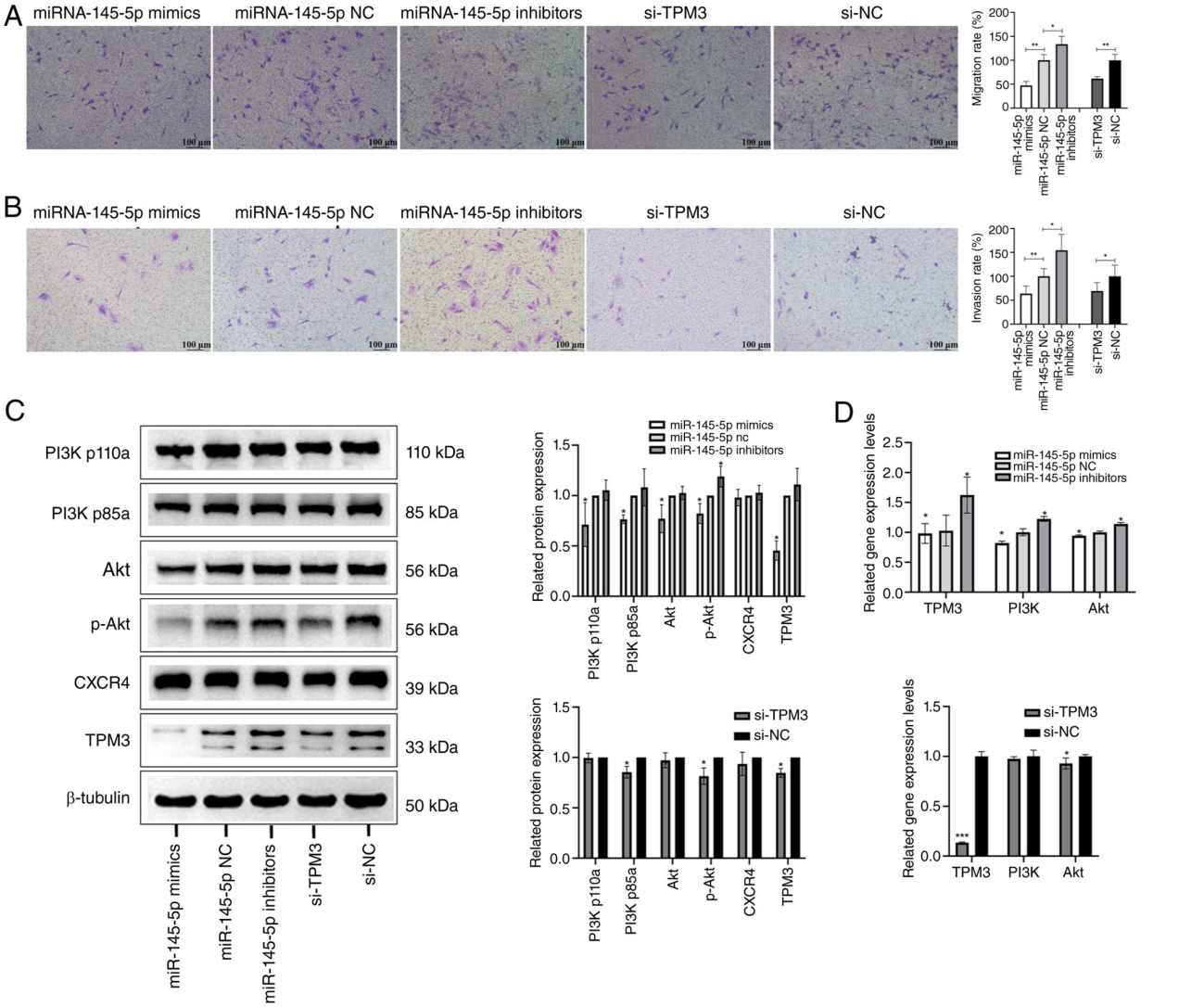

Figure 6. Effects of treatment on migration, invasion and associated gene expression changes in papillary thyroid cancer cells. (A) Cell migration ability of each group detected by Transwell assay. (B) Cell invasion ability of each group detected by Transwell assay. (C) Expression levels of associated proteins in each group determined by western blotting. (D) Relative mRNA expression levels of associated genes in each group measured using reverse transcription-quantitative PCR. *P<0.05 and **P<0.01 miR-145-5p mimics/inhibitors group vs. miR-145-5p NC group; si-*TPM3* group vs. si-NC group. miR, microRNA; TPM3, tropomyosin 3; si, small interfering; NC, negative control; p-, phosphorylated.

investigated the molecular mechanism by which exosomal miR-145-5p suppresses PTC progression by targeting *TPM3*, thereby providing a novel theoretical basis for targeted therapy of thyroid cancer.

The primary finding of the present study was that plasma exosomal miR-145-5p levels were significantly elevated in patients with PTC compared with those harboring benign thyroid nodules, whereas TCGA data revealed downregulated miR-145-5p expression in PTC tissues. This paradoxical expression pattern underscores the unique biological complexity of miR-145-5p in PTC. At the tissue level, the present results correspond with those of previous reports. Boufraqech *et al* (27) demonstrated that miR-145 is markedly downregulated in thyroid cancer tissues and cell lines and that its overexpression suppresses tumor growth and metastasis through direct targeting of Akt3. Subsequent studies have consistently demonstrated the low expression of miR-145-5p in PTC tissues (28-30). In addition, Boufraqech *et al* (27) also found that at the circulating/exosomal level, serum miR-145 levels were elevated in patients with thyroid cancer and exhibited a venous gradient. Samsonov *et al* (9) further reported that numerous miRNAs, including miR-145-5p, were highly expressed in preoperative plasma exosomes of patients with PTC and that their levels declined notably at 7-10 days after tumor resection, suggesting an association with tumor burden. Notably, recent work has indicated that miRNA signals in extracellular compartments (such as circulation and exosomes) are do not just mirror tissue molecular profiles, but represent independently transformed and coordinately regulated networks specific to each compartment (31). Based on this conceptual framework, two potential mechanisms are proposed: i) Plasma exosomal miR-145-5p may be predominantly secreted by non-tumor cells, such as immune cells and stromal cells, thereby exerting an endocrine-mediated inhibitory effect on thyroid cancer cell proliferation and invasion; and ii) tumor cells themselves may actively secrete exosomal miR-145-5p to modulate their own cellular state, thereby restoring or maintaining tumor stemness and facilitating

malignant progression. This dual-source hypothesis not only reconciles the tissue-low vs. plasma-high discrepancy but also aligns with the complexity of intercellular communication within the tumor microenvironment.

To identify the functional downstream targets of miR-145-5p, cross-prediction was performed using the TargetScan and mirDIP databases, and experimentally validated *TPM3* as a direct functional target of miR-145-5p. *TPM3*, a member of the tropomyosin family, fuses with the neurotrophic receptor tyrosine kinase gene to generate tyrosine receptor kinase oncogenes, representing one of the known driver genetic alterations in PTC (32). Aberrant *TPM3* expression (including both oncogenic fusion-driven activation and dysregulated overexpression) has been implicated in PTC pathogenesis (33). The present study revealed that *TPM3* is significantly upregulated in thyroid cancer tissues and its expression is associated with lymph node metastasis, tumor stemness and immune infiltration, thereby expanding the pathological significance of *TPM3* in PTC. Importantly, a number of previous studies have identified other functional targets of miR-145-5p in PTC. Feng *et al* (28) demonstrated that long non-coding RNA n384546 acts as a competing endogenous RNA for miR-145-5p to regulate *Akt*, thereby promoting PTC proliferation, invasion and metastasis. Chen *et al* (34) reported that miR-145 inhibits PTC cell migration and invasion through the NF-κB pathway; Wen *et al* (35) demonstrated that miR-145 targets Ras-associated protein Rab-5c (Rab5c) and modulates the MAPK/ERK pathway to suppress TPC-1 cell proliferation and invasion. Han *et al* (36) recently showed that circular_pleckstrin and sec 7 domain-containing protein 3 functions as a competing endogenous RNA that sponges miR-145-5p/miR-338-3p to regulate the high mobility group box 3 (*HMGB3*) axis, driving PTC proliferation, migration, invasion and epithelial-mesenchymal transition. The identification of *TPM3* in the present study, together with previously reported targets, such as *Akt, Rab5c* and *HMGB3*, suggests that miR-145-5p uses a multi-target synergy strategy to exert its tumor-suppressive functions. It may preferentially engage different downstream targets in response to distinct biological contexts or cell types. Furthermore, *TPM3* has been established as a prognostic biomarker in cervical cancer, where it is associated with immune infiltration (13). *TPM3* overexpression induces epithelial-mesenchymal transition in pancreatic cancer (14), indicating that the oncogenic role of *TPM3* is conserved across a number of cancer types. The present *in vitro* functional experiments, which showed that *TPM3* knockdown notably suppresses PTC cell proliferation, migration and invasion, are consistent with these cross-cancer findings, further consolidating *TPM3* as a potential therapeutic target in PTC.

At the mechanistic level, it was determined that miR-145-5p directly targets *TPM3*, thereby inhibiting activation of the PI3K-Akt signaling pathway. The PI3K-Akt axis is a core signaling cascade that broadly regulates tumor cell proliferation, energy metabolism and angiogenesis and its aberrant activation is well-recognized as a hallmark of malignant progression in numerous cancers, including breast, lung, colorectal and thyroid cancers (37). The present results are corroborated within a study by Boufraqech *et al* (27), which showed that miR-145 overexpression suppresses the PI3K/Akt pathway by directly targeting Akt3. The distinction lies in the fact that Boufraqech *et al* (27) identified direct targeting of the terminal effector Akt3, whereas the present study revealed that miR-145-5p can indirectly inhibit this pathway through targeting an upstream regulator such as *TPM3*. This suggests that miR-145-5p used a multi-layered regulatory mode, acting at upstream and downstream nodes of the PI3K-Akt cascade. This observation is also comparable with the findings in other cancers: In oral squamous carcinoma, miR-145-5p overexpression similarly suppresses PI3K/Akt activity (38). Despite the intermediate targets differing across cancer types (namely neuroblastoma Ras viral oncogene homolog and *TPM3*), the convergent suppression of PI3K-Akt signaling suggests that this pathway may serve as a core hub for the tumor-suppressive function of miR-145-5p. Regarding the precise mechanism by which TPM3 modulates PI3K-Akt activity, it is hypothesized that *TPM3*, as an actin-binding protein, may regulate cytoskeletal remodeling, thereby affecting integrin-mediated signal transduction or the clustering and activation of growth factor receptors on the plasma membrane, which in turn modulates the input strength of upstream signals to PI3K-Akt. This hypothesis warrants further investigation using co-immunoprecipitation and membrane fractionation assays.

Furthermore, the association between *TPM3* and the tumor immune microenvironment was explored. Correlation analyses showed that *TPM3* expression was significantly correlated with the majority of immune regulatory genes and immune checkpoint molecules, and positively correlated with infiltration of Tregs, NK cells and CAFs. However, at the single-cell level in the TPC-1 cells, miR-145-5p overexpression and *TPM3* knockdown did not exhibit notable changes in C-X-C motif chemokine receptor 4 (*CXCR4*) expression, which was selected for experimental validation from the panel of immune regulatory receptors analyzed in the bioinformatics screening (data not shown). Therefore, it is proposed that *TPM3* may not directly regulate intrinsic *CXCR4* expression in PTC cells but may indirectly modulate the overall *CXCR4* profile by remodeling immune cell infiltration patterns within the tumor microenvironment. This inference is consistent with the present bioinformatics finding that *TPM3* expression is positively correlated with immune infiltration scores, but it requires further validation in co-culture systems or animal models.

The present study exhibits a number of limitations. All *in vitro* experiments were performed exclusively in the TPC-1 PTC cell line without functional or mechanistic verification in additional PTC cell lines; this may have limited the generalizability of conclusions. In addition, the cellular origin of plasma exosomal miR-145-5p has not been clarified by lineage-tracing experiments and detailed mechanisms by which *TPM3* modulates the immune microenvironment remain to be elucidated. Future studies should aim to incorporate numerous PTC cell lines and use animal models and clinical tissue samples to further validate the core findings. Single-cell sequencing and spatial transcriptomics should also be utilized to further investigate the precise role of the exosomal miR-145-5p/*TPM3* axis in tumor-immune crosstalk.

In conclusion, the present study demonstrates that exosomal miR-145-5p inhibits *TPM3* expression, thereby downregulating PI3K-Akt signaling and ultimately suppressing the

proliferation, migration and invasion of PTC cells. The present findings not only reveal a novel mechanism of the miR-145-5p/*TPM3* axis in PTC progression but also provide a potential new target and theoretical foundation for molecular targeted therapy of thyroid cancer.

Acknowledgements

Not applicable.

Funding

The present study was supported by the Natural Science Foundation of Shandong Province (grant nos. ZR2021MH328 and ZR2022QH096) and the General Program of the Special Project for Cultivation and Improvement of Military Traditional Chinese Medicine Service Capacity (grant no. 2023ZY059).

Availability of data and materials

The data generated in the present study may be requested from the corresponding author.

Authors' contributions

YW conducted the investigation, formal analysis and writing of the original draft. XC was responsible for conceptualization and writing, reviewing and editing the manuscript. WS participated in the acquisition of data. QH contributed to the study design, data interpretation, funding acquisition, project supervision and reviewed and approved the final version of the manuscript. YW and XC confirm the authenticity of all the raw data. All authors read and approved the final version of the manuscript.

Ethics approval and consent to participate

The human umbilical cord mesenchymal stem cells used in this study were obtained from discarded umbilical cords of mothers who delivered at the 960th Hospital of the PLA Joint Logistics Support Force. Sample collection was approved by the hospital's ethics committee (approval no. 2024 044) and written informed consent was obtained from all donors. Exosome isolation and subsequent experiments were performed within the scope of the approved research protocol.

Patient consent for publication

Not applicable.

Competing interests

The authors declare that they have no competing interests.

References

1. Diao X, Guo C, Jin Y, Li B, Gao X, Du X, Chen Z, Jo M, Zeng Y, Ding C, *et al*: Cancer situation in China: An analysis based on the global epidemiological data released in 2024. Cancer Commun (Lond) 45: 178-197, 2025.
2. Boucai L, Zafereo M and Cabanillas ME: Thyroid cancer: A review. JAMA 331: 425-435, 2024.
3. van Niel G, D'Angelo G and Raposo G: Shedding light on the cell biology of extracellular vesicles. Nat Rev Mol Cell Biol 19: 213-228, 2018.
4. Debbi L, Guo S, Safina D and Levenberg S: Boosting extracellular vesicle secretion. Biotechnol Adv 59: 107983, 2022.
5. Li Q, He G, Yu Y, Li X, Peng X and Yang L: Exosome crosstalk between cancer stem cells and tumor microenvironment: Cancer progression and therapeutic strategies. Stem Cell Res Ther 15: 449, 2024.
6. Lee JC, Zhao JT, Gundara J, Serpell J, Bach LA and Sidhu S: Papillary thyroid cancer-derived exosomes contain miRNA-146b and miRNA-222. J Surg Res 196: 39-48, 2015.
7. Tang M, Wang Q, Wang K and Wang F: Mesenchymal stem cells-originated exosomal microRNA-152 impairs proliferation, invasion and migration of thyroid carcinoma cells by interacting with DPP4. J Endocrinol Invest 43: 1787-1796, 2020.
8. Lu J, Liu X, Cen A, Hong Y and Wang Y: HYPOXIA induces lncRNA HOTAIR for recruiting RELA in papillary thyroid cancer cells to upregulate miR-181a and promote angiogenesis. J Endocrinol Invest 47: 2873-2884, 2024.
9. Samsonov R, Burdakov V, Shtam T, Radzhabova Z, Vasilyev D, Tsyrlina E, Titov S, Ivanov M, Berstein L, Filatov M, *et al*: Plasma exosomal miR-21 and miR-181a differentiates follicular from papillary thyroid cancer. Tumour Biol 37: 12011-12021, 2016.
10. Chen J, Chen T, Zhu Y, Li Y, Zhang Y, Wang Y, Li X, Xie X, Wang J, Huang M, *et al*: circPTN sponges miR-145-5p/miR-330-5p to promote proliferation and stemness in glioma. J Exp Clin Cancer Res 38: 398, 2019.
11. Tang W, Zhang X, Tan W, Gao J, Pan L, Ye X, Chen L and Zheng W: miR-145-5p suppresses breast cancer progression by inhibiting SOX2. J Surg Res 236: 278-287, 2019.
12. Agarwal V, Bell GW, Nam JW and Bartel DP: Predicting effective microRNA target sites in mammalian mRNAs. Elife 4: e05005, 2015.
13. Chen A, Li S, Guo C, Gu C, Gui J, Deng Y, Feng X and Mi Y: Tropomyosin 3 gene fusions in cancers: From mechanisms to treatments-a comprehensive review. Cancer Med 14: e71407, 2025.
14. Gatalica Z, Xiu J, Swensen J and Vranic S: Molecular characterization of cancers with NTRK gene fusions. Mod Pathol 32: 147-153, 2019.
15. Zhao YC, Wang TJ, Qu GH, She LZ, Cui J, Zhang RF and Qu HD: TPM3: A novel prognostic biomarker of cervical cancer that correlates with immune infiltration and promotes malignant behavior in vivo and in vitro. In: Am J Cancer Res 15: 3123-3139, 2023.
16. Zhou S, Ma X, Wang ZJ, Zhang WY, Jiang H, Li SD, Zhang TZ, Du J and Lu Z: Research on the establishment of a TPM3 monoclonal stable transfected PANC-1 cell line and the experiment of the EMT occurrence in human pancreatic cancer. Onco Targets Ther 12: 5577-5587, 2019.
17. Yoshihara K, Shahmoradgoli M, Martínez E, Vegesna R, Kim H, Torres-Garcia W, Treviño V, Shen H, Laird PW, Levine DA, *et al*: Inferring tumour purity and stromal and immune cell admixture from expression data. Nat Commun 4: 2612, 2013.
18. Li T, Fu J, Zeng Z, Cohen D, Li J, Chen Q, Li B and Liu X: TIMER2.0 for analysis of tumor-infiltrating immune cells. Nucleic Acids Res 48: W509-W514, 2020.
19. Racle J, de Jonge K, Baumgaertner P, Speiser DE and Gfeller D: Simultaneous enumeration of cancer and immune cell types from bulk tumor gene expression data. Elife 6: e26476, 2017.
20. Newman AM, Liu CL, Green MR, Gentles AJ, Feng W, Xu Y, Hoang CD, Diehn M and Alizadeh AA: Robust enumeration of cell subsets from tissue expression profiles. Nat Methods 12: 453-457, 2015.
21. Aran D, Hu Z and Butte AJ: xCell: Digitally portraying the tissue cellular heterogeneity landscape. Genome Biol 18: 220, 2017.
22. Livak KJ and Schmittgen TD: Analysis of relative gene expression data using real-time quantitative PCR and the 2(-Delta Delta C(T)) method. Methods 25: 402-408, 2001.
23. Welsh JA, Goberdhan DCI, O'Driscoll L, Buzas EI, Blenkiron C, Bussolati B, Cai H, Vizio DD, Driedonks TAP, Erdbrügger U, *et al*: Minimal information for studies of extracellular vesicles (MISEV2023): From basic to advanced approaches. J Extracell Vesicles 13: e12404, 2024.
24. Nair GC, Sekhar SR, Menon RR, Jacob P, Babu MJC and Pillai AV: Ten-year outcome of papillary thyroid carcinoma, the efficacy of risk stratification systems in predicting long-term adverse outcomes. Indian J Cancer 63: 35-40, 2026.

25. Ma T, Xie Y, Long X and Ye F: High risk factors, molecular features and clinical management for radioactive iodine-refractory differentiated thyroid carcinoma. Front Oncol 15: 1644562, 2025.
26. Xu Z, Chen Y, Ma L, Chen Y, Liu J, Guo Y, Yu T, Zhang L, Zhu L and Shu Y: Role of exosomal non-coding RNAs from tumor cells and tumor-associated macrophages in the tumor microenvironment. Mol Ther 30: 3133-3154, 2022.
27. Boufraqech M, Zhang L, Jain M, Patel D, Ellis R, Xiong Y, He M, Nilubol N, Merino MJ and Kebebew E: miR-145 suppresses thyroid cancer growth and metastasis and targets AKT3. Endocr Relat Cancer 21: 517-531, 2014.
28. Feng J, Zhou Q, Yi H, Ma S, Li D, Xu Y, Wang J and Yin S: A novel lncRNA n384546 promotes thyroid papillary cancer progression and metastasis by acting as a competing endogenous RNA of miR-145-5p to regulate AKT3. Cell Death Dis 10: 433, 2019.
29. Ruiz-Pozo VA, Cadena-Ullauri S, Guevara-Ramírez P, Paz-Cruz E, Tamayo-Trujillo R and Zambrano AK: Differential microRNA expression for diagnosis and prognosis of papillary thyroid cancer. Front Med (Lausanne) 10: 1139362, 2023.
30. Li X, Tian Y, Hu Y, Yang Z, Zhang L and Luo J: CircNUP214 sponges miR-145 to promote the expression of ZEB2 in thyroid cancer cells. Biochem Biophys Res Commun 507: 168-172, 2018.
31. Kallinikas G, Ektesabi AM, Vaswani CM, Haronis G, Kallinika E, Kozyrakis D, Rodinos E, Filios A, Filios P, Mityliniou D, *et al*: A brief review of microRNA profiling in human prostate cancer tissues and plasma. Biomolecules 15: 1156, 2025.
32. Pekova B, Sykorova V, Mastnikova K, Vaclavikova E, Moravcova J, Vlcek P, Lastuvka P, Taudy M, Katra R, Bavor P, *et al*: NTRK fusion genes in thyroid carcinomas: Clinicopathological characteristics and their impacts on prognosis. Cancers (Basel) 13: 1932, 2021.
33. Greco A, Miranda C and Pierotti MA: Rearrangements of NTRK1 gene in papillary thyroid carcinoma. Mol Cell Endocrinol 321: 44-49, 2010.
34. Chen Q, Zhou L, Ye X, Tao M and Wu J: miR-145-5p suppresses proliferation, metastasis and EMT of colorectal cancer by targeting CDCA3. Pathol Res Pract 216: 152872, 2020.
35. Wen X, Yan Z, Du J, Dai J, Liu M, Wang X and Wang N: Effects of miR-145 targeting rab5c and regulating MAPK/ERK signaling pathway on proliferation and invasion of thyroid papillary carcinoma cells. Cell Mol Biol (Noisy-le-grand) 69: 44-47, 2023.
36. Han P, Chen G, Zhang Q, Shen W, Li M and Lv J: Circ_PSD3 stimulates cell proliferation, migration, invasion and epithelial to mesenchymal transition (EMT) in papillary thyroid carcinoma via the regulation of miR-145-5p/miR-338-3p/HMGB3 axis. J Biochem Mol Toxicol 39: e70402, 2025.
37. Yip HYK and Papa A: Signaling pathways in cancer: Therapeutic targets, combinatorial treatments, and new developments. Cells 10: 659, 2021.
38. Zhou J and Jin S: Circ_0058063 contributed to oral squamous cell carcinoma development by sponging miR-145 and regulating PI3K/AKT pathway. Mol Biotechnol 65: 2049-2060, 2023.